AIRESEARCH QCGAT ENGINE – ACOUSTIC TEST RESULTS

Larry S. Kisner
AiResearch Manufacturing Company of Arizona
A Division of The Garrett Corporation

SUMMARY

The noise levels of the AiResearch Quiet, Clean, General Aviation Turbofan (QCGAT) engine were measured in ground static noise tests. The static noise levels were found to be markedly lower than the demonstrably quiet AiResearch Model TFE731 engine. The measured QCGAT noise levels were correlated with analytical noise-source predictions to derive free-field component noise predictions. These component noise sources were used to predict the QCGAT flyover noise levels at FAR Part 36 conditions. The predicted flyover noise levels are about 10 decibels lower than the current quietest business jets.

INTRODUCTION

This paper describes the acoustic design, static noise test results, noise source correlation analyses, and flyover noise predictions for the AiResearch QCGAT engine.

NOISE GOALS

NASA specified goals for the QCGAT engine at the FAR Part 36 sideline, takeoff, and approach conditions as a function of maximum takeoff gross weight. The noise goals for the twin-engine airplane postulated in this program are shown in figure 1. The maximum takeoff gross weight for the airplane defined by AiResearch is 8674 kg (19,122 lb). The specific noise goals at the FAR Part 36 conditions are:

Takeoff (without cutback):	73.3 EPNdB
Sideline (1500 ft):	82.3 EPNdB
Approach:	87.3 EPNdB

These levels are significantly below the existing FAR Part 36 Stage 3 noise limits.

NOISE OBJECTIVES

To achieve the program noise objectives, large turbofan engine noise-reduction technology was applied to the smaller AiResearch general aviation engine. The objectives accomplished during the program were as follows:

o   The engine was defined, and the cycle conditions were determined to provide low noise-generation features.

o   An acoustically treated nacelle was designed and fabricated.

o   The ground static engine noise levels were measured for several configurations, establishing an engine baseline and demonstrating the effectiveness of the acoustical design features.

o   Static noise-source correlations were developed, and component noise spectra with adjustments for flight effects were used to estimate flyover noise levels in compliance with QCGAT noise goals.

ACOUSTIC DESIGN FEATURES

The acoustic design effort emphasized minimizing noise generation at the source and maximizing noise reduction achieved through

judicious application of nacelle acoustic treatment in the fan inlet and exhaust ducts. Acoustic duct liner configurations were designed to balance the noise suppression at takeoff, sideline, and approach condition, providing the broadest possible attenuation bandwidth without sacrificing significant attenuation from optimum at any one of the three operating conditions.

The major acoustic features of the QCGAT engine are illustrated in figure 2. Noise-reduction technology was applied to the two major noise sources, the fan and the jet. The fan noise-source reduction features included the following: elimination of inlet guide vanes, low tip speed and pressure ratio, single-stage fan, a large rotor to stator spacing of 2.12 rotor chords, and a large number of bypass and core stators to cut-off rotor-stator interaction tones. The jet noise-reduction features included low fan discharge and primary jet-exhaust velocities, and a 12-lobe mixer compound exhaust nozzle.

The nacelle acoustic treatment design selected for the QCGAT engine consisted of a single-cavity system used in series with different cavity depths in the axial direction and where possible equivalent depths on opposing walls. A broadband resonator was constructed from aluminum perforated sheet bonded to a 0.95-cm (3/8-in.) all-aluminum honeycomb backing because of its structural ruggedness, low cost, and known acoustic performance.

A schematic of the acoustic liner installation is shown in figure 3. The inlet-wall treatments--sections A_1, A_2, and B--were tuned to provide primary suppression at the FAR Part 36 sideline condition with a length equal to 2.16-cm (0.85-in.) mean inlet diameter. The fan discharge duct treatments--sections 1, 2, and 3--were tuned to provide balanced attenuation between sideline and approach conditions, and have an effective total length equal to 5.4 times the average duct height.

Final optimization of the engine and nacelle exhaust liner design was completed using a computer program based upon the axisymmetric mode theory of Minner and Rice (ref. 1). To achieve optimum attenuation, the required cavity depths and face sheet open areas were computed.

The design procedure for the inlet liners was based upon the recent multimodal duct treatment analysis developed at NASA-Lewis by Rice (ref. 2 through 5). The inlet liners were tuned to attenuate modes that radiate energy at larger angles from the inlet axis, thus reducing sideline noise radiation.

The major design characteristics of the inlet and exhaust liners are shown in table 1. The inlet sections A_1, A_2, and B have backing depths of 1.83 cm (0.72 in.), 2.8 cm (1.1 in.), and 1.35 cm (0.53 in.), respectively. Open areas range from 5.8 to 14.2 percent. The inlet liners are tuned for the sideline condition in the 1000- to 2500-Hz range. The total length of the inlet treatment is 59.9 cm (23.6 in.). The exhaust liner configuration is 123.7-cm (48.7-in.) long and was tuned for approach conditions where fan exhaust noise is dominant in the 2000- to 4000-Hz frequency range.

ENGINE NOISE TESTS

The QCGAT engine was installed at the AiResearch San Tan test facility (fig. 4) for acoustical measurements. Noise data was taken at specified engine load conditions from ground idle to take-off power to determine the untreated engine noise levels, the noise reduction attained with various combinations of acoustic treatments, and the noise reduction achieved with a mixer compound exhaust nozzle. This data was used to determine the static noise levels for use in predicting flyover noise levels.

A schematic of the acoustic test setup at San Tan is shown in figure 5. Data was taken on a 30.4-meter (100-foot) radius at every 10 degrees, from 10 degrees to 160 degrees, for each configuration and load condition. The microphones are B&K, 1.270-cm (0.5-in.) diameter, Type 4133, mounted for normal incidence of the direct sound field and were located 1.5 meters (5 ft) above the ground.

In addition to the 16 far-field microphone locations, 6 internal noise measurements were made with three 0.3175-cm (0.125-in.) condensor microphones and three 0.6350-cm (0.25-in.) condensor infinite tube systems (fig. 6). Two 0.3175-cm (0.125-in.) microphones were installed flush mounted with the duct surface in the fan inlet nacelle, one near the fan tip, the other near the nacelle inlet. Another 0.32-cm (0.125-in.) microphone was located in the exhaust duct near the mixer exit plane. The 0.6350-cm (0.25-in.) infinite tube systems were located in the low-pressure (LP) turbine rear-bearing support area aft of the LP turbine, near the mixer exit plane, and near the exhaust nozzle exit plane. The internal noise measurements were recorded simultaneously with the far-field measurements. This data was recorded for 2 minutes at each condition to allow coherence analysis between the internal and far-field noise.

All tests were conducted within the recommended environmental limits of wind speed, temperature, and relative humidity. The tests were conducted in November 1978 from midnight to 6 a.m. when the wind was calm and ambient noise levels were low. The temperature ranged from 280K (44°F) to 286K (56°F) and the relative humidity ranged from 70 to 85 percent during the tests.

The key acoustic parameters for the simulated static takeoff and approach conditions are shown in table 2. At takeoff, the engine operates at 16,098 N (3619 lb) of thrust with a fan pressure

ratio of 1.41. The fan relative tip Mach number is supersonic at 1.17, and the mixer exhaust velocity is only 258 m/s (846 ft/sec). The fan-blade passing frequency is 5236 Hz, in a low annoyance range.

At approach, the fan operates subsonically at a relative tip Mach number of 0.79. The fan pressure ratio is 1.18, and the fan-blade passing frequency is 3638 Hz. The thrust level at approach, static condition, is 7019 N (1578 lb) with a lower mixer exhaust velocity of 166 m/s (545 ft/sec).

Table 3 shows the same key acoustic parameters of the FAR Part 36 flight conditions of takeoff, sideline, and approach. Tables 2 and 3 show a comparison between static and flight fan relative tip Mach numbers and jet velocities. At takeoff, the QCGAT airplane reaches an altitude of 1151 m (3776 ft) above measurement location. At this altitude, thrust is at 12,869 N (2893 lb), with a fan pressure ratio of 1.44. The fan relative tip Mach number is 1.22, and blade passing frequency is 5495 Hz. Mixer exhaust velocity is 285 m/s (936 ft/sec). At approach, the fan relative tip Mach number is 0.78, the fan pressure ratio is 1.16, and the blade passing frequency is 3677 Hz. At a thrust level of 4639 N (1043 lb), the mixer exhaust velocity is 176 m/s (577 ft/sec). Sideline acoustic parameters are essentially the same as takeoff acoustic parameters.

Acoustic data was taken for the seven test configurations listed in table 4. The fully treated engine was tested first with both mixer compound and coannular exhaust nozzle systems (configurations 1 and 2). With the mixer nozzle installed, acoustic panels were systematically replaced with hardwall panels in configurations 3 and 4 until the fully hardwall configuration 5 was attained. Configuration 6 was the hardwall engine with the nacelle lip instead of the flight-simulator lip. The final configuration, configuration 7, consisted of the hardwall nacelle, flight-simulator lip, and coannular nozzle. Comparisons were made between

the treated and hardwall with mixer compound nozzle (configuration 1 versus 5), treated and hardwall with coannular nozzle (configuration 2 versus 7), mixer compound versus coannular nozzle with treated nacelle (configuration 1 versus 2), and mixer compound versus coannular nozzle with hardwall nacelle (configuration 5 versus 7).

GROUND REFLECTION ANALYSIS

Before the ground static acoustic data can be compared or used to predict flyover noise levels, the data must be corrected for FAA 248K (77°F) and 70-percent relative humidity, and for ground reflection. The ground reflection problem is illustrated in figure 7. A wave reflected from the ground interferes with the direct sound wave at the receiver. Depending on ground acoustic impedance, the reflected wave can diminish or enhance the sound intensity at the microphone due to a phase-angle shift. The type of soil at the San Tan site consists of a random combination of hard-packed clay, sand, and decomposed granite particles; no known data exists on the impedance of this soil.

The terrain around San Tan Cell No. 5 slopes downward from the engine pad so that the ground locations upon which the microphones were pole-mounted are at an average elevation of 1.13 m (3.7 ft) below that of the engine pad. Thus, the QCGAT engine, which was mounted 2.29 m (7.5-ft) above the engine pad was, on the average, 3.41 m (11.2-ft) above the ground, relative to the microphone locations.

The impedance correlation procedure, based upon references 6 through 13, is outlined as follows:

1. Measured data at takeoff condition at all three microphone heights and all 16 array angles were used to obtain final AiResearch San Tan soil impedance estimates.

71

2. Using previously published data, an initial normalized impedance array was assumed ($R/\rho c$ and $X/\rho c$ versus frequency).

3. The excess attenuation, A_e, was computed for each microphone height, and corrected sound pressure level (SPL_c) spectra was determined.

4. A 3-way difference scheme was used to calculate the differences between the three corrected spectra at each 1/3-octave band.

5. Iterations were performed on the values of $R/\rho c$ and $X/\rho c$ until all differences approached zero (steps 3 and 4, above). The convergence criteria was based upon the values of average differences at each 1/3-octave band. When reasonable values of impedance failed to provide convergence at a 1/3-octave band, the two microphone heights having a frequency furthest away from a null frequency were used and convergence was obtained.

6. Inasmuch as convergence criteria was based on average differences, observations of individual differences were then made, and minor adjustments to the normalized impedance were performed, thus establishing the final impedance values given in figure 8.

7. Excess attenuation 1/3-octave band spectra was computed for the three microphone heights, based on final ground impedance estimates.

8. A_e spectra was then applied to the measured data for all three microphone heights. Comparison plots were prepared at representative array angles.

9. Acoustic measurements were also made at the three microphone heights for approach. To check the relative validity of the ground-reflection correction procedure, the A_e spectra was applied to the approach data and comparisons of the corrected data again were made. The correlation of the approach corrected data was consistent with that of the takeoff corrected data.

An example of the 'as measured' spectra from each microphone is shown in figure 9. Large differences between the pole-mounted and ground microphones were observed from 200 to 4000 Hz. Figure 10 shows the same data with the excess attenuation corrections applied. Overall, good agreement was obtained for all microphones and all 1/3-octave band frequencies.

An example of the final result of applying the ground correction is shown in figure 11. The free-field levels were reduced in the low frequency range, and the ground dip in the 400- through 500-Hz range was decreased, resulting in a smooth spectral curve. Little or no change occurred at the high frequencies.

ACOUSTIC COMPARISONS OF STATIC DATA

The corrected data for each acoustic configuration tested was compared to establish trends and illustrate the level comparisons with the equivalent Model TFE731-3 takeoff and approach static data. A comparison between the hardwall coannular configuration--the loudest QCGAT configuration--with the Model TFE731-3 at takeoff condition is shown in figure 12. The QCGAT tone-corrected perceived noise levels (PNLT) are considerably lower than the Model TFE731-3 primarily because of the lower exhaust velocity, even though the QCGAT engine produces 8-percent more thrust. This difference is shown more vividly in the 1/3-octave spectral plot at 150 degrees from the inlet axis (fig. 13). This shows clearly a

reduction in jet noise, as well as in the high frequency fan tone. Similar reductions were achieved at approach.

Further reductions in noise were achieved with the QCGAT mixer compound nozzle as shown in figure 14. At the same 150-degree angle, the QCGAT coannular and mixer compound nozzle configurations are compared at takeoff static condition. At 200 Hz, the mixer is about 7 dB quieter than the coannular nozzle. Note, however, that there are peaks at 1600 and 2500 Hz with the mixer being 2- to 3-dB higher at these frequencies. The source of these tones were investigated in detail, including some cross-correlation analysis at NASA. The results revealed a high correlation between internal core noise and the far-field noise levels at certain discrete frequencies, primarily centered about 200 Hz and 2500 Hz. This led to the development of a new noise-source correlation attributing this excess noise to core noise.

Final reductions in noise were attained with the acoustically treated mixer configuration as shown in figure 15. Also shown in figure 15 is the treated versus hardwall mixer data at approach condition and at 50 degrees from the fan inlet. A broad range of frequencies from 630 Hz to 6300 Hz are attenuated due to the inlet treatment. The same configurations are compared at 120 degrees in the aft quadrant in figure 16. Here, larger attenuations approaching 10 dB are observed, but in a narrower frequency band. The actual attenuations in the lower frequencies cannot be observed because of the masking by jet and core noise sources.

The treatment was effective in reducing the sideline noise levels as shown in figure 17. The treated versus hardwall coannular configurations at 90 degrees and at approach condition are shown. The blade passing tone at 4000 Hz is attenuated nearly 7 dB.

In summarizing ground static data comparisons, the AiResearch QCGAT engine demonstrated significantly quieter noise levels than the currently quiet Model TFE731 business-jet engine, and showed that application of noise reduction technology, such as a mixer compound exhaust system and acoustically treated fan inlet and exhaust nacelles, achieved even lower noise levels.

NOISE SOURCE CORRELATIONS

A primary objective of the QCGAT acoustic program was to determine flyover noise levels based on static engine data, and to demonstrate that these noise levels meet the program goals, which are set well below current technology airplane. To accomplish this objective, a methodology was derived to predict the major component noise sources, adjust the individual sources from static to flight conditions, and predict the noise source flyover levels.

The analytical tools used by AiResearch to predict QCGAT engine noise sources are presented in table 5. The prediction procedures for fan noise, jet noise, and core noise were based upon the NASA Aircraft Noise Prediction Program (ANOPP) recommended procedures with empirical modifications based upon previous AiResearch experience.

A comparison of predicted noise sources based upon these prediction procedures and measured data is shown in figure 18. The fan noise prediction agrees well with the measured data with a slight overprediction of the blade passing harmonic. However, the measured low-frequency noise, particularly from 160 Hz to 2500 Hz, is higher than predicted jet and core noise. In order to account for this, it is necessary to make assumptions for the apportionment of the jet and core to the total noise signature. Two approaches were used and are shown in table 6: The first model attributed the difference between predicted and measured noise in the 50- to

2500-Hz frequency range to the jet. Jet noise was adjusted accordingly on an average delta basis. The second model assumed jet noise predictions were valid, and adjusted the core noise to exactly match the measured data. Both models adjusted the fan and turbine noise to exactly match the measured levels in the appropriate frequency range.

Figure 19 shows an example of the jet-noise-dominated correlation for the softwall mixer at 120 degrees and at takeoff condition. The average difference from 50 to 2000 Hz is applied at each frequency to produce a modified jet noise prediction that fairs through the data. In this model, core noise is predicted to be well below the jet noise at the takeoff condition. Above 2000 Hz, the fan noise is adjusted to fit the data. Turbine noise contributions were unimportant except at frequencies above 12,500 Hz, which was out of the range of interest for flyover noise calculations. Similar correlations were made for each far-field angle from 10 to 160 degrees.

The same set of acoustic data is shown in figure 20, with the core-noise-dominated model predictions. The jet noise prediction is considerably below the measured data. The fan noise was determined to be the difference between the measured total and the predicted sum of jet, core, and turbine noise in the 3150- to 10,000-Hz bands. The total of all the noise sources exactly matched the measured data.

FLYOVER PREDICTION PROCEDURE

Calculated flyover noise levels for the QCGAT engine were based upon the adjusted noise sources obtained from correlating the predicted and measured static noise data. A block diagram of this procedure is given in figure 21. The measured corrected static noise data and the predicted noise sources are fed into a program

called NASADELTA. The program compares and computes difference spectra for each noise source at each engine operating condition. The noise source prediction program is again used to predict the noise levels at the FAR Part 36 flyover conditions. These predictions are adjusted by applying the appropriate correction spectra determined from the static data.

The adjusted noise sources are taken to flight conditions with corrections for distance, atmospheric attenuation, jet relative velocity and dynamic amplification effects, fan inlet cleanup, doppler effects, wing shielding, and ground effects. The adjusted sources are "flown" along a prescribed flight path using the GTENFLY program.

For each flyover condition -- takeoff, sideline, and approach-- the SPL, PNL, and PNLT were calculated for each 1/2 second of the flight trajectory. The duration time, duration correction, effective perceived noise level (EPNL) for each source, and the total EPNL were calculated in accordance to FAR Part 36 procedures.

FLYOVER NOISE CALIBRATION WITH MEASURED LEARJET DATA

Based upon static data comparisons, the QCGAT engine demonstrated substantial reductions in noise levels compared to the quiet AiResearch Model TFE731-2 engine that powers the Learjet 35/36 airplane. This airplane is certified to be 5 EPNdB below the FAR Part 36 Stage 3 noise limits. However, the initial flyover predictions, based upon the previously described methodology, yielded QCGAT noise levels comparable to measured Learjet flyover noise levels. This methodology was thus used to predict the Learjet flyover noise levels to determine its validity.

A comparison of the predicted and measured in-flight spectra for the Learjet 35/36 based upon the excess jet noise model, is

shown in figure 22. Although the static noise predictions for the TFE731 engine were adjusted to match measured static noise levels, when taken to flight, the predictions are higher than the measured flyover levels. The overprediction occurs primarily in the low frequency, jet-dominated range. At the takeoff condition, the predicted flyover EPNL is 88.7 EPNdB compared to a measured value of 84 EPNdB. Similar differences between predicted and measured flyover noise levels were observed at approach and sideline conditions.

A second set of flyover predictions for the Learjet certification tests were made based upon the core noise dominated model, as shown in figure 23. The predicted levels are even higher than those based upon the previous model. This is primarily due to the assumed dominance of core noise to which beneficial in-flight reductions are not applied.

Table 7 compares the predicted and measured total EPNL for takeoff and approach conditions for both prediction models. The individual noise sources cannot be compared directly because the flight-path position for which the maximum tone-corrected perceived noise level occurs is not the same, resulting in a different composition of noise sources. This shift in location of the maximum PNLT prevents the use of an in-flight spectral difference array to match the measured flyover data. The spectral correction model was abandoned in favor of a single EPNL correction delta applied to each source. An outline of this calibration procedure used to match the measured Learjet data and to predict the QCGAT flyover noise levels is shown in figure 24. The final QCGAT flyover noise levels reflect measured flyover data and are thus considered realistic.

QCGAT FLYOVER NOISE PREDICTIONS

The unadjusted and adjusted flyover noise predictions for the QCGAT engine are given in table 8. Each method, with appropriate adjustments for differences between predicted and measured Learjet levels yielded similar results, indicating that the QCGAT engine is 2.0 EPNdB below the sideline noise goal, 4.6 to 5.4 EPNdB below the approach noise goal, and from 0.2 EPNdB below to 1.4 EPNdB above the takeoff noise goal.

ACOUSTIC ANALYSIS SUMMARY

A summary of the acoustic analysis performed in the QCGAT program is outlined below:

o   A ground reflection analysis was developed to correct the measured static noise levels to free-field.

o   Flyover noise predictions were made based upon two separate noise source correlation models: One assumed jet noise to be the dominant generating mechanism; the other assumed core noise to be responsible for excess noise above the known jet noise levels.

o   Both prediction models were applied to the TFE731-2-powered Learjet and were found to overpredict the measured in-flight levels, although the ground static data was used to calibrate the predictions.

o   The overpredictions occurred primarily in the low-frequency range where both jet and core noise are expected to be important.

o   Final flyover predictions were made with adjustments for
     the differences between predicted and measured Learjet
     noise levels.

SUMMARY OF ACOUSTIC RESULTS

The noise reduction technology demonstrated in the QCGAT Pro-
gram is summarized below:

o   The QCGAT softwall nacelle/mixer configuration demon-
     strated a 9.3 EPNdB reduction in flyover noise at takeoff
     condition, a 10.3 EPNdB reduction at approach, and a 7.7
     EPNdB reduction at sideline condition compared to the
     TFE731-2-powered Learjet.

o   The QCGAT hardwall nacelle coannular nozzle configura-
     tion was shown to be 4.2 EPNdB quieter than the Learjet
     at takeoff condition, although the QCGAT airplane takeoff
     gross weight is 963 kg (2122 lb) greater than the
     Learjet.

o   The QCGAT hardwall nacelle/mixer was 3.5 EPNdB quieter at
     takeoff and 4.3 EPNdB quieter at approach than the QCGAT
     hardwall nacelle/coannular nozzle.

o   The QCGAT softwall nacelle/mixer was quieter than the
     QCGAT hardwall nacelle/mixer by 2.6 EPNdB and 1.3 EPNdB
     at approach and takeoff conditions, respectively.

The final QCGAT flyover noise levels based upon the excess
core noise model are shown in figures 25 through 27, compared with
the FAR Part 36 noise limits, the QCGAT noise goals, and the mea-
sured Learjet flyover levels.

CONCLUSIONS

The measured static noise levels of the AiResearch QCGAT engine were markedly lower than the demonstrably quiet TFE731 engine. The following conclusions were made:

o   Based on the excess jet noise correlation model, the QCGAT engine met or bettered the program noise goals.

o   Based on the excess core noise correlation, the QCGAT engine met or bettered the program noise goals both for hardwall and softwall nacelle configurations at sideline and approach conditions, and was slightly above the take-off noise goal.

The AiResearch QCGAT program has demonstrated that it is possible to design quiet engines for general aviation aircraft.

REFERENCES

1. Minner, G.L. and Rice, E.J., "Computer Method for Design of Acoustic Liners for Turbofan Engines," NASA TM X-3317, 1976.

2. Rice, E.J., "Acoustic Liner Optimum Impedance for Spinning Modes with Mode Cut-Off Ratio as the Design Criterion," AIAA Paper 76-516, Palo Alto, CA., 1976.

3. Rice, E.J., "Inlet Noise Suppressor Design Method Based Upon the Distribution of Acoustic Power with Mode Cut-Off Ratio," Paper Presented at the Thirteenth Annual Meeting of the Society of Engineering Science, Inc., George Washington University, 1976.

4. Rice, E.J., "Multimodal Far-Field Acoustic Radiation Pattern -An Approximate Equation," AIAA Paper 77-1281, presented in Atlanta Georgia, October, 1977.

5. Rice, E.J., "Attenuation of Sound in Ducts with Acoustic Treatment - A Generalized Approximate Equation," NASA TMX-71830.

6. Pao, S.P., A.R. Wenzel, and P.B. Oncely, "Prediction of Ground Effects on Aircraft Noise," NASA-TP-1104, 1978.

7. Zorumski, W.E., "Prediction of Aircraft Sideline Noise Attenuation," NASA-TM-78717, 1978.

8. Chessell, C.I., "Propagation of Noise Along a Finite Impedance Boundary," J. Acoust. Soc. America, Vol. 62, No. 4, October 1977, pp. 825-834.

9. Chessell, C.I., "Meteorological and Ground Effects on the Propagation of Aircraft Noise Close to the Earth's Surface," Jl. of Sound and Vib., Vol. 60, No. 2, 1978, pp. 251-266.

10. Embleton, T.F.W., J.E. Piercy, and N. Olson, "Outdoor Sound Propagation Over Ground of Finite Impedance," J. Acoust. Soc. Am., Vol. 59, No. 2, February 1976, pp. 267-277.

11. Daigle, G.A., Effects of Atmospheric Turbulence on the Interface of Sound Waves Above a Finite Impedance Boundary," J. Acoust. Soc. Am., Vol. 65, No. 1, January 1979, pp. 45-49.

12. Putnam, T.W., "Review of Aircraft Noise Propagation," NASA-TMX-56033, September, 1975.

13. Oncely, P.B., "Propagation of Jet Engine Noise Near a Porous Surface," J. Sound Vib., Vol. 13, No. 1, 1970, pp. 27-35.

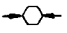## TABLE 1. QCGAT NACELLE ATTENUATOR DESIGN CHARACTERISTICS.

Liner Section	Tuned Freq, Hz	Operating Condition Tuned for	Liner Length, cm (in.)	Face Sheet Open Area, %	Cavity Depth, cm (in.)	Honeycomb Cell Size, cm (in.)
A$_1$	1000	Sideline	17.5(6.9)	5.8	18.83(0.72)	1.905(0.75)
A$_2$	1000	Sideline	27.2(10.7)	8.6	2.79(1.10)	1.905(0.75)
B	2500	Sideline	15.2(6.0)	14.2	1.32(0.52)	0.953(0.375)
1	2500	Approach	32.0(12.6)	7.0	1.42(0.56)	0.953(0.375)
2	4000	Approach	38.9(15.3)	8.6	0.91(0.36)	0.953(0.375)
3	2000	Approach	52.8(20.8)	6.8	1.96(0.77)	1.905(0.75)

TABLE 2. QCGAT ENGINE KEY ACOUSTIC PARAMETERS FOR SIMULATED STATIC TEST CONDITION.

Engine Parameter	Simulated Static Test Condition, 282K (48°F)	
	Takeoff	Approach
Engine net thrust	16,098 N (3,619 lbf)	7,019 N (1,578 lbf)
Fan rotor speed	913 rad/s (8,726 rpm)	634.8 rad/s (6,063 rpm)
Fan pressure ratio, tip	1.41	1.18
Fan tip relative Mach No.	1.17	0.79
Fan blade passing frequency	5,236 Hz	3,638 Hz
Fan airflow	61.7 kg/s (136.1 lbm/sec)	42.4 kg/s (93.5 lbm/sec)
Core airflow	11.6 kg/s (25.5 lbm/sec)	6.2 kg/s (13.6 lbm/sec)
Mixer exhaust velocity	257.9 m/s (846 ft/sec)	166.1 m/s (545 ft/sec)
Mixer exhaust total temperature	406.8K (732.3°R)	365.9K (658.6°R)
LP turbine rotor speed	1,941.5 rad/s (18,543 rpm)	1,348.9 rad/s (12,883 rpm)
Turbine last stage relative tip Mach No.	0.472	0.349
Turbine last stage pressure ratio (total to static)	1.61	1.22

TABLE 3. QCGAT ENGINE KEY ACOUSTIC PARAMETERS FOR FLYOVER NOISE CONDITION.

Engine Parameter	FAR PART 36 CERTIFICATION CONDITION		
	Takeoff	Sideline	Approach
Engine net thrust	12,869 N (2,893 lbf)	13,318 N (2,994 lbf)	4,639 N (1,043 lbf)
Fan rotor speed	958.9 rad/s (9,159 rpm)	954.8 rad/s (9,119 rpm)	641.4 rad/s (6,126 rpm)
Fan pressure ratio, tip	1.44	1.43	1.16
Fan tip relative Mach No.	1.22	1.20	0.78
Fan blade passing frequency	5,495 Hz	5,471 Hz	3,677 Hz
Fan airflow	60.1 kg/s (132.4 lbm/sec)	62.4 kg/s (137.6 lbm/sec)	44.8 kg/s (98.7 lbm/sec)
Core airflow	11.4 kg/s (25.2 lbm/sec)	11.9 kg/s (26.3 lbm/sec)	6.2 kg/s (13.7 lbm/sec)
Mixer exhaust velocity	285.3 m/s (936 ft/sec)	284.3 m/s (933 ft/sec)	175.9 m/s (577 ft/sec)
Mixer exhaust total temperature	429.1K (772.3°R)	433.8K (780.8°R)	381.5K (686.7°R)
LP turbine rotor speed	2,037.8 rad/s (19,463 rpm)	2,028.9 rad/s (19,378 rpm)	1,363.3 rad/s (13,021 rpm)
Turbine last stage relative tip Mach No.	0.467	0.465	0.356
Turbine last stage pressure ratio (total to static)	1.70	1.69	1.26

TABLE 4. ACOUSTIC TEST CONFIGURATIONS.

Acoustic Configuration Number	Description
1	Fully treated engine with mixer compound nozzle
2	Fully treated engine with coannular nozzle
3 & 4	Partially treated with mixer compound nozzle
5	Hardwall engine with mixer compound nozzle
6	Hardwall engine with nacelle lip, mixer nozzle
7	Hardwall engine with coannular nozzle

TABLE 5.   QCGAT ENGINE NOISE PREDICTION PROCEDURE.

Major Component Noise Sources Predicted	Prediction Method
Fan inlet noise – Discrete, broadband	NASA TMX-71763*
Buzz saw	FAA-RD-71-73*
Fan discharge noise – Discrete, broadband	NASA TMX-71763*
Jet noise	NASA TMX-73552
Combustion noise	NASA TMS-71627
Turbine noise	AIAA 75-449
Total noise	Sum of individual component noise levels

NOTE: One-third octave spectra from 50 to 16,000 Hertz
        directivity angles from 0.17 to 2.79 radians
        (10 to 160 degrees) from inlet centerline.

*Modified by AiResearch

TABLE 6.   NOISE PREDICTION METHODOLOGY COMPARISON.

Excess Jet Model	Excess Core Model
Jet noise based on NASA method adjusted to fair through low-frequency data	Jet noise based on NASA method
Core noise based on NASA method	Core noise defined as difference between measured and predicted sum of jet, fan, turbine in 50-250 Hz frequency bands
Fan discrete, broadband, and buzz saw adjusted to 731 data	Fan inlet and fan discharge defined as difference between measured and predicted sum of jet, core, turbine in 3150-10,000 Hz bands
GE turbine noise method	GE turbine noise method

TABLE 7. TFE731-2/LEAR 36 FLYOVER NOISE COMPARISON.

| | EPNL, EPNdB | | |
| | Predicted | | Measured |
	Excess Jet Model	Excess Core Model	
Takeoff	88.7 (+4.7)	90.8 (+6.8)	84.0
Approach	95.9 (+3.7)	98.6 (+6.4)	92.2

TABLE 8. QCGAT FLYOVER NOISE SUMMARY.

| Configuration | EPNL, EPNdB | | | | QCGAT Goal |
| | Excess Jet Prediction Method | | Excess Core Prediction Method | | |
	Unadjusted	With Lear △	Unadjusted	With Lear △	
Hardwall mixer takeoff	79.3	74.6	83.1	76.0	
Softwall mixer takeoff	77.8	73.1 (-0.2)*	81.7	74.7 (+1.4)*	73.3
Hardwall mixer approach	88.2	84.5	91.0	84.5	
Softwall mixer approach	86.4	82.7 (-4.6)*	88.5	81.9 (-5.4)*	87.3
Hardwall mixer sideline	85.7	81.7	89.0	81.7	
Softwall mixer sideline	84.3	80.3 (-2.0)*	87.6	80.3 (-2.0)*	82.3

*Indicates difference between goal and predicted EPNL.

86

TAKEOFF POINT
73.3 EPNdB

6.48 km (3.5 NMI)

1828.8 m (6000 FT)

1828.8 m (6000 FT)

SIDELINE NOISE POINTS*
82.3 EPNdB

1828.8 m (6000 FT)

113 m (370 FT) ALTITUDE

0.052 rad (3°)

0.46 km (0.25 NMI) SIDELINE

1.85 km (1.0 NMI)

APPROACH POINT
87.3 EPNdB

*SIDELINE NOISE LEVEL BASED ON HIGHEST LEVEL OCCURING AT THE THREE SIDELINE POINTS.
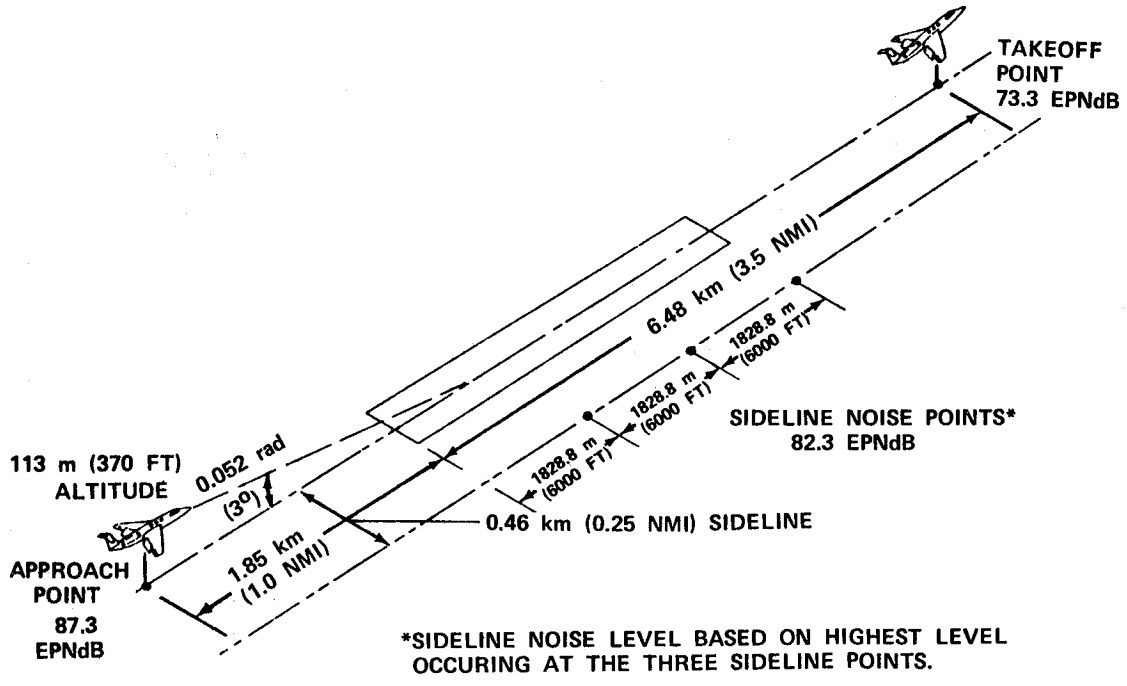
Figure 1. QCGAT Airplane Noise Goals.

121 BYPASS VANES

73 CORE VANES

FAN EXHAUST DUCT ACOUSTICAL TREATMENT (L/H = 5.4)

LOW FAN JET VELOCITY

LOW TIP SPEED SINGLE-STAGE FAN 36 BLADES

LOW PRIMARY JET VELOCITY

MIXER-COMPOUND NOZZLE

NO INLET GUIDE VANES

INLET ACOUSTICAL TREATMENT (L/D = 0.85)

LARGE ROTOR-STATOR SPACING ROTOR-STATOR NUMBERS SELECTED TO CUT-OFF INTERACTION TONES
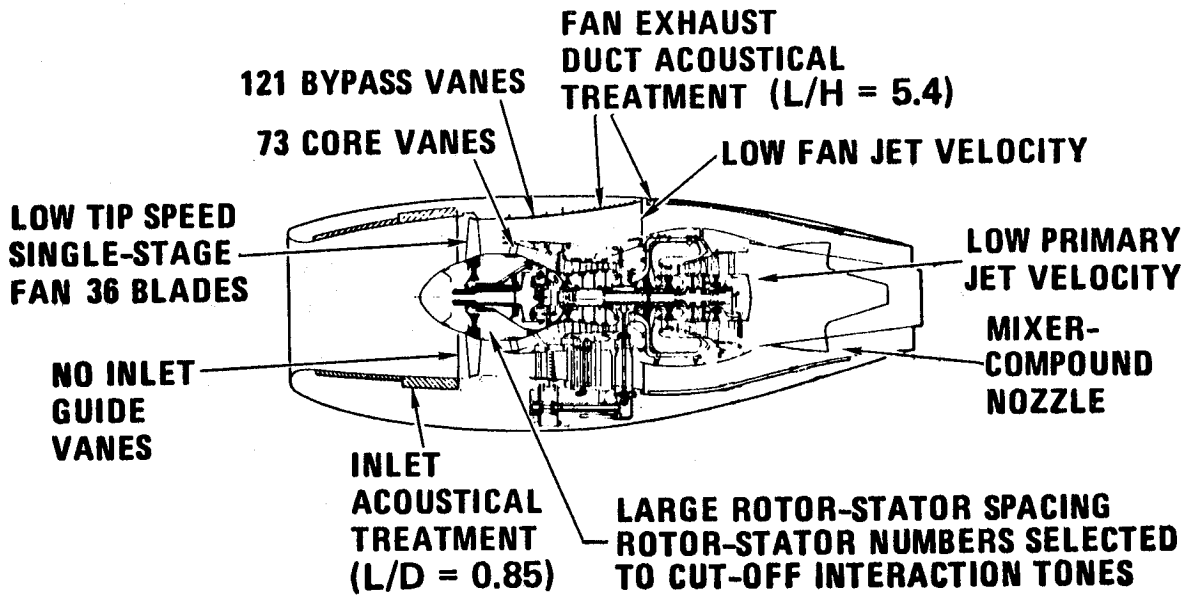
Figure 2. QCGAT Acoustic Design Features.

ATTENUATOR LENGTH, cm (IN.)
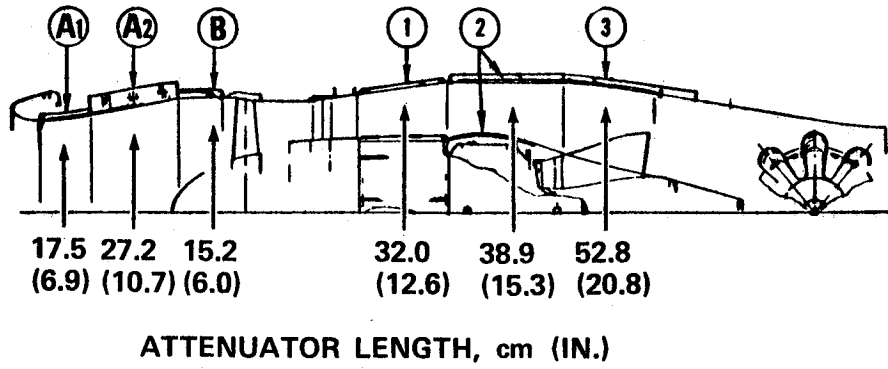
NOTE:

◯ DENOTES SECTION NUMBER USED
IN ATTENUATION ANALYSIS

Figure 3.   Nacelle Acoustic Treatment.

Figure 4.   San Tan Acoustic Test Site.

ANGLE FROM
ENGINE INLET
CENTERLINE 0.175 RAD (10°)
0.349 RAD (20°)
0.524 RAD (30°)
0.698 RAD (40°)
0.873 RAD (50°)
1.047 RAD (60°)
1.222 RAD (70°)
1.396 RAD (80°)
1.571 RAD (90°)
1.745 RAD (100°)
1.910 RAD (110°)
2.094 RAD (120°)
2.069 RAD (130°)
2.443 RAD (140°)
2.618 RAD (150°)
2.793 RAD (160°)

MICROPHONE
LOCATION NO.

CONCRETE
ASPHALT
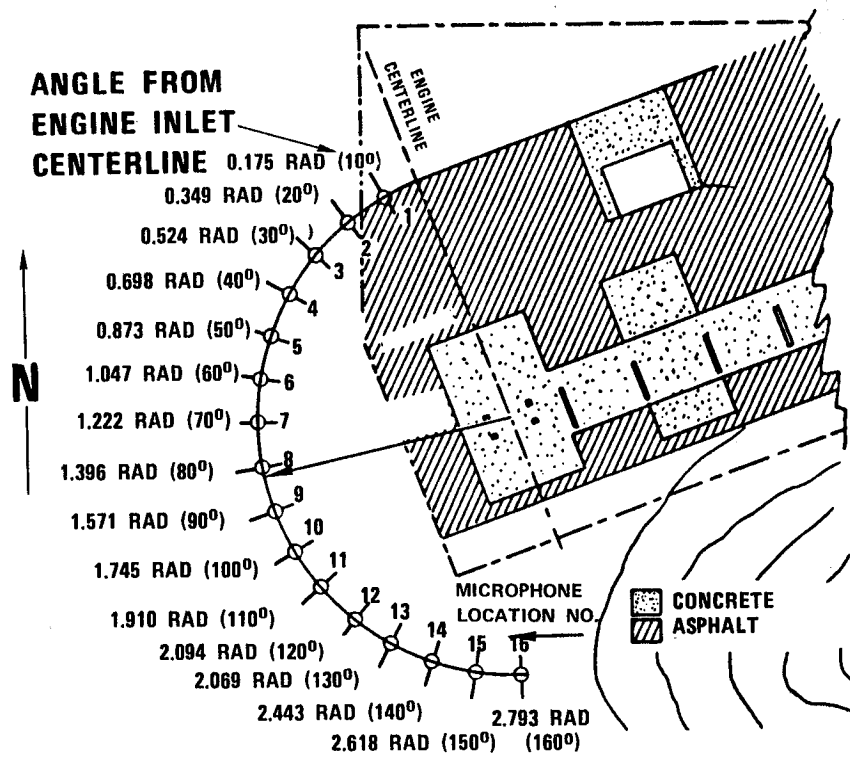
Figure 5. Acoustic Test Setup.
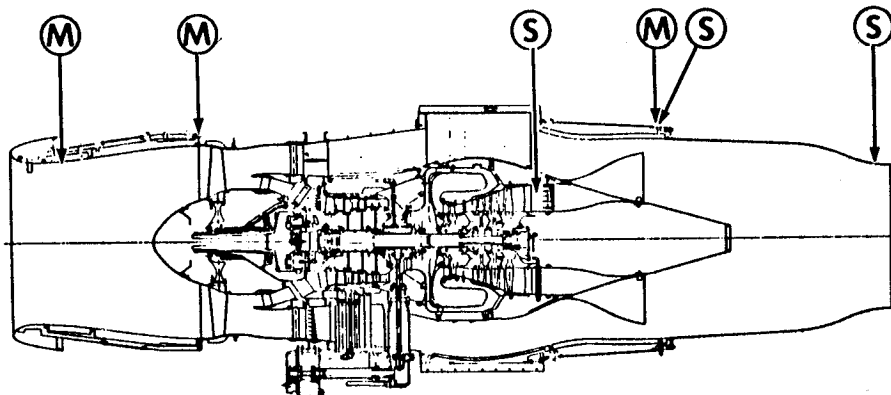
Ⓜ DENOTES 0.3175-cm (1/8-IN.) MICROPHONE

Ⓢ DENOTES 0.635-cm (1/4-IN.) SEMI-INFINITE TUBE

Figure 6. Internal Acoustic Instrumentation.
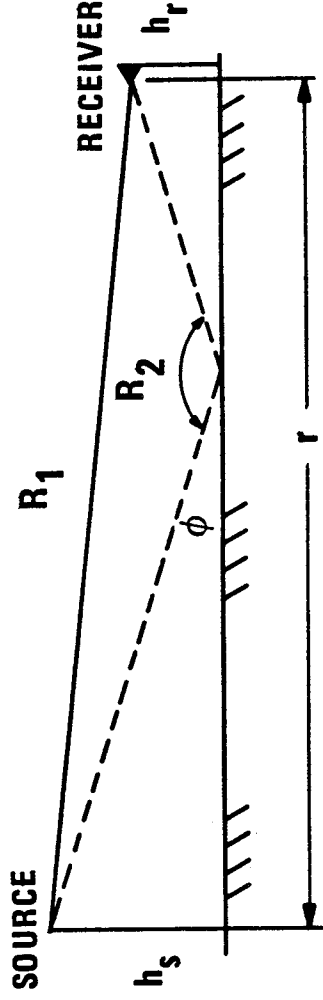
Figure 7. Ground Reflection Correction Model.
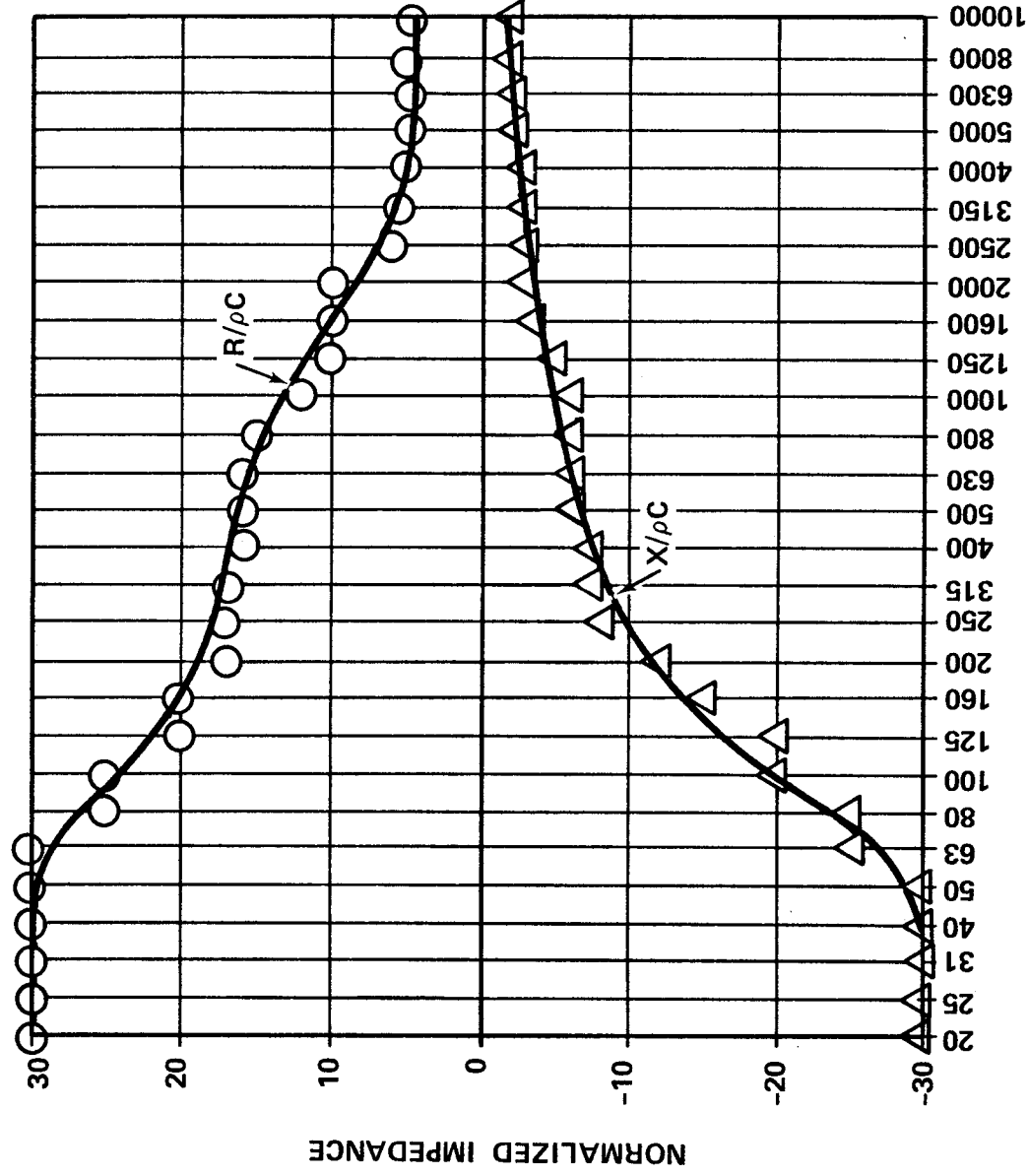
ONE-THIRD OCTAVE BAND CENTER FREQUENCIES - Hz

Figure 8. Correlated Acoustic Impedance for Desert Soil at San Tan (AiResearch).

90
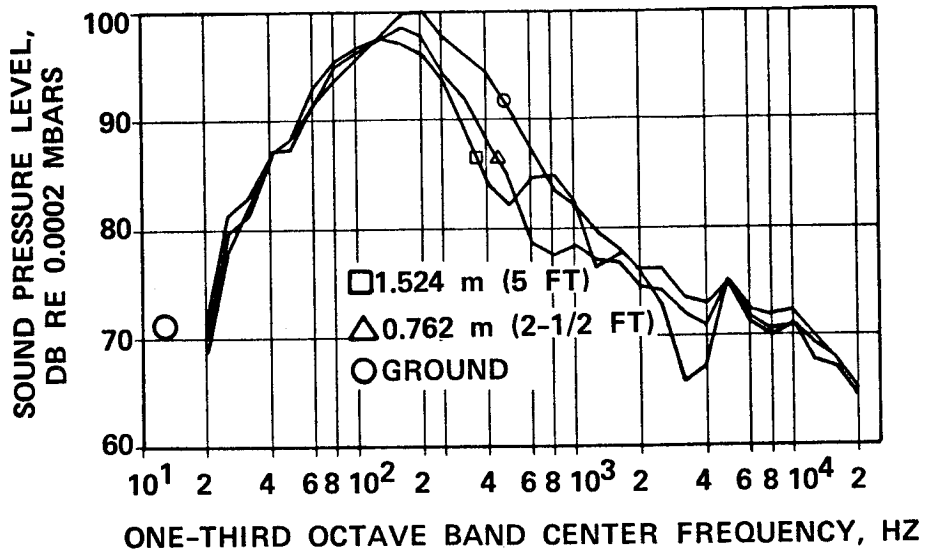
Figure 9. Measured Data for Acoustic Configuration No. 2 at 2.62 Radian (150-Degree) Position.
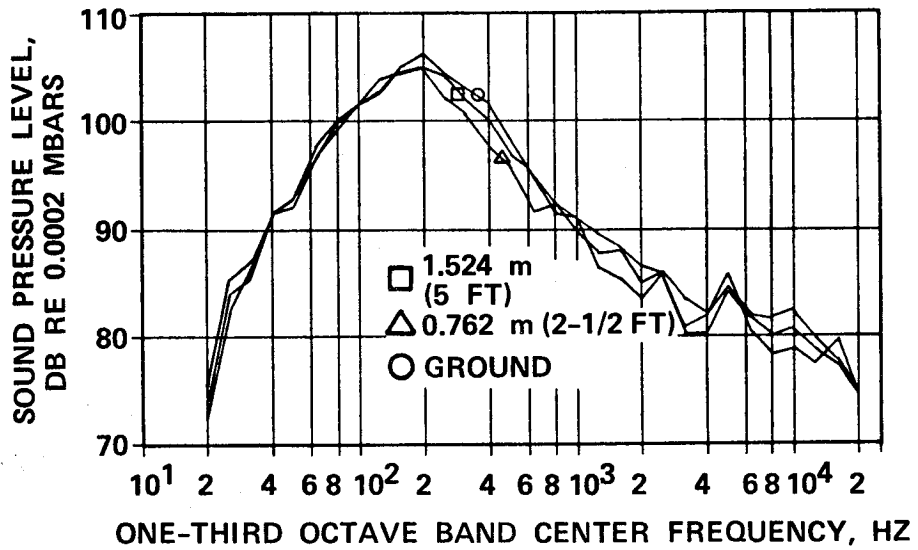
Figure 10. Corrected Data for Acoustic Configuration No. 2 at 2.62 Radian (150-Degree) Position.

30.48 m (100 FT) RADIUS
MIKE HEIGHT: 1.524 m (5 FT)
AT 2.62 rad (150°)

——— RAW DATA
－－－CORRECTED DATA
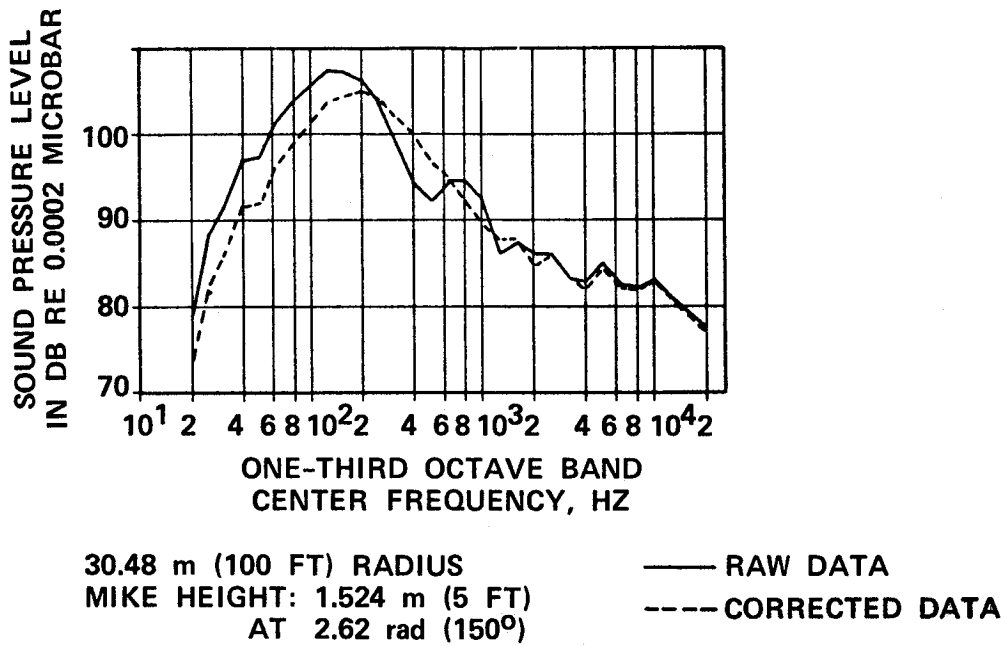
Figure 11. Raw Data versus Ground Corrected Data.

O TFE731-3 RUN 9

△ QCGAT CF708C
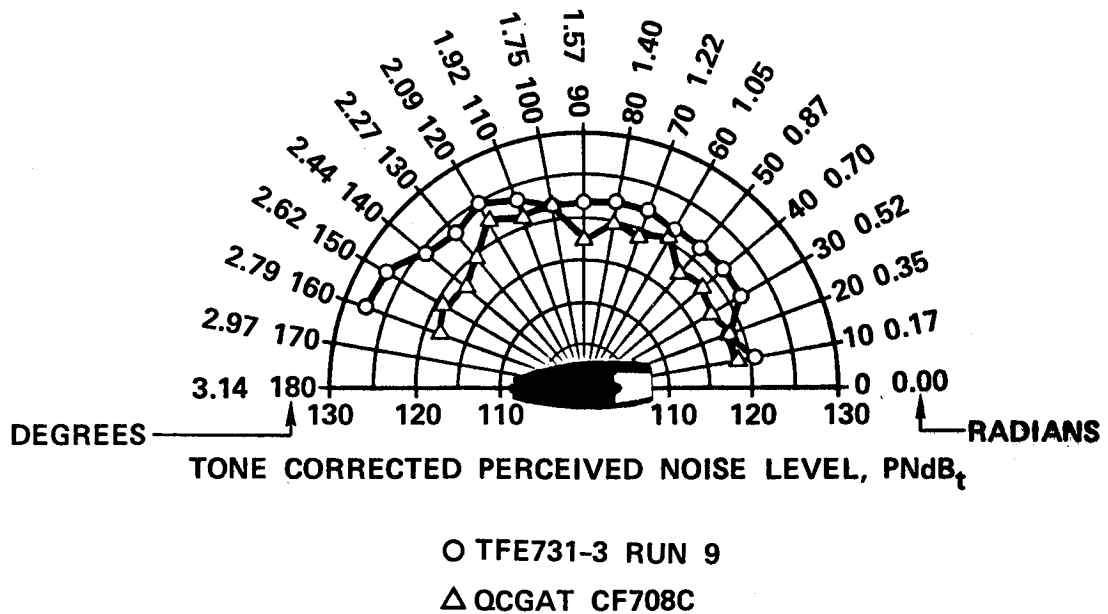
Figure 12. Static Comparison at Takeoff of Model TFE731-3
and QCGAT Coannular Nozzle Configurations.
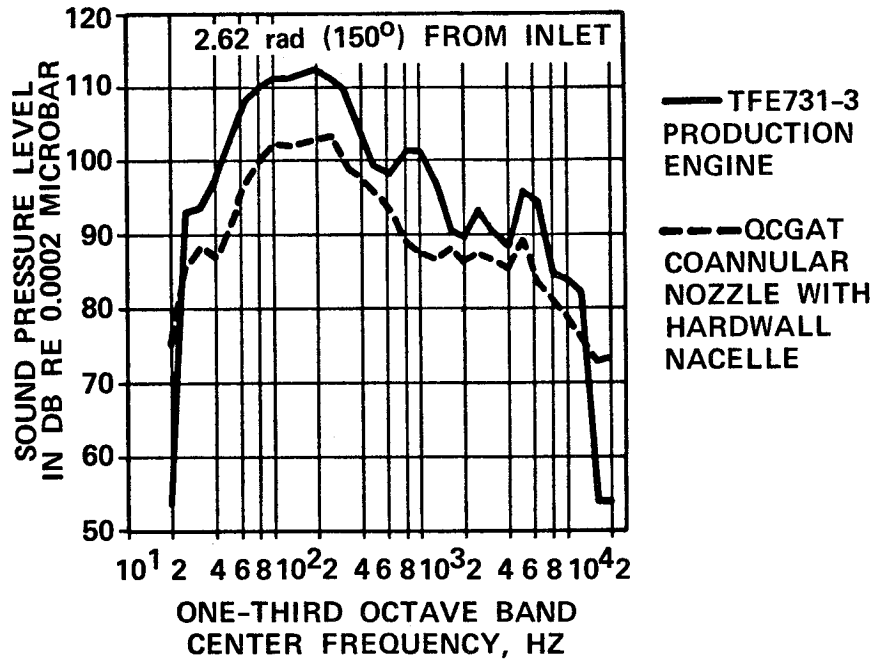
Figure 13. Noise Level Comparison at Takeoff
of Model TFE731 and QCGAT Coannular
Nozzle Configurations.
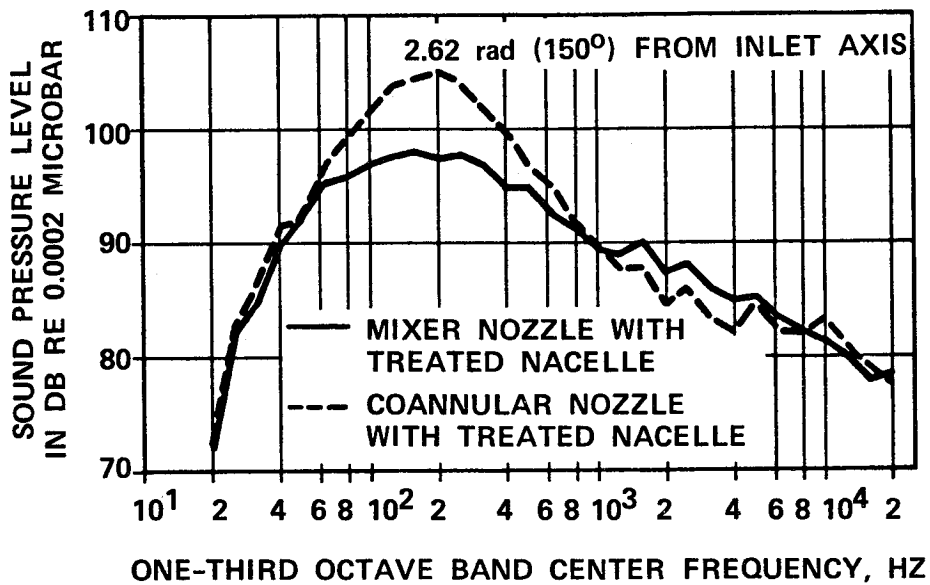
Figure 14. Noise Level Comparison at Takeoff
of QCGAT Mixer Compound and
Coannular Nozzle Configurations.

0.87 rad (50°) FROM INLET

SOUND PRESSURE LEVEL IN DB RE 0.0002 MICROBAR

—— HARDWALL NACELLE
– – – TREATED NACELLE

ONE-THIRD OCTAVE BAND CENTER FREQUENCY, HZ
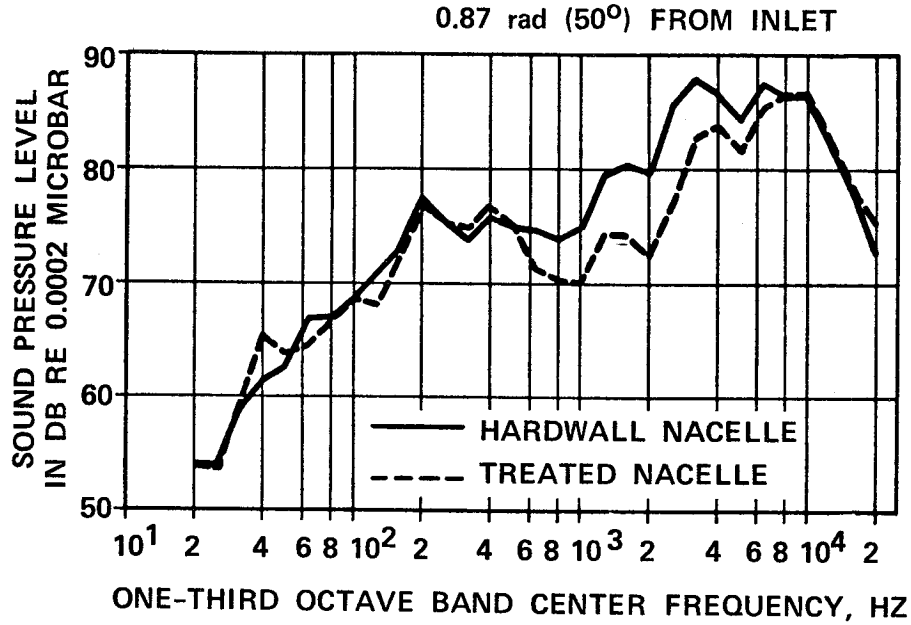
Figure 15. Approach Noise Level Comparison of Hardwall versus Treated Acoustic Panels at 0.87 rad (50°) from Engine Inlet Centerline for the Mixer Compound Nozzle Configuration.

2.09 rad (120°) FROM INLET

SOUND PRESSURE LEVEL IN DB RE 0.0002 MICROBAR

—— HARDWALL
– – – TREATED

ONE-THIRD OCTAVE BAND CENTER FREQUENCY, HZ
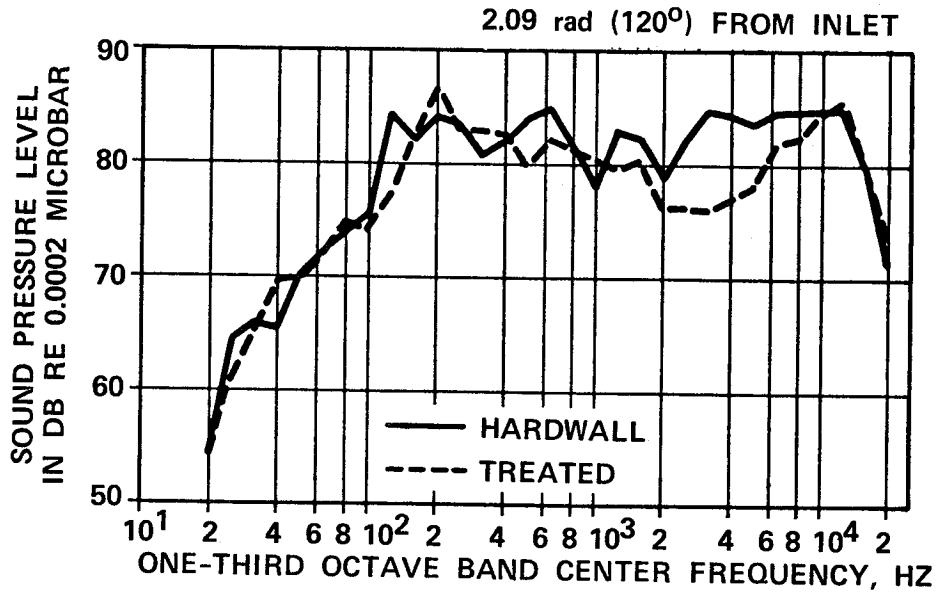
Figure 16. Approach Noise Level Comparison of Hardwall versus Treated Acoustic Panels at 2.09 rad (120°) from Engine Inlet Centerline for the Mixer Compound Nozzle Configuration.
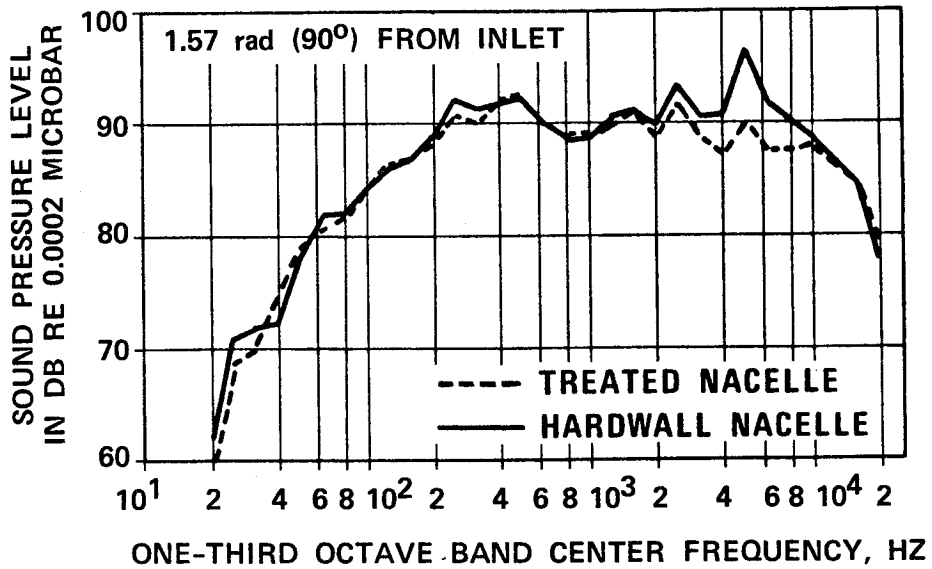
Figure 17. Takeoff Noise Level Comparison of Hardwall versus
Treated Acoustic Panels at 1.57 rad (90°) from
Engine Inlet Centerline for the Coannular Nozzle
Configuration.
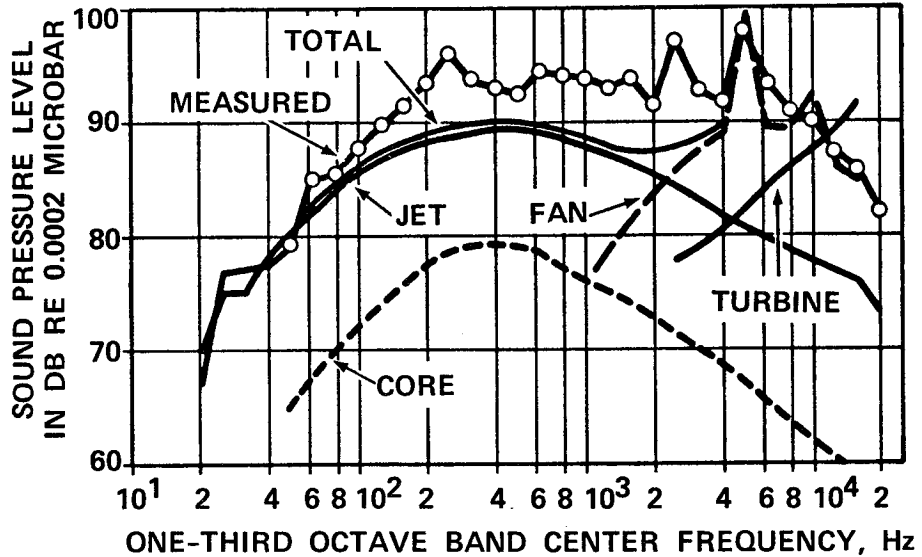
Figure 18. Comparison of Measured and Predicted
Noise Levels Before Correlation.
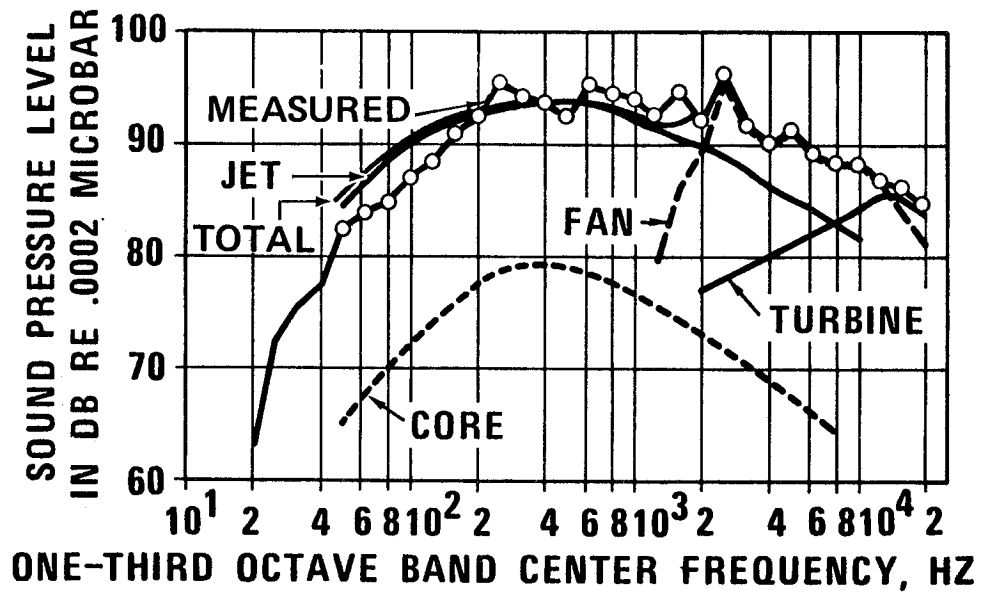
Figure 19. Data Correlation, Excess Jet Model,
Softwall Mixer, 2.09-Radian
(120-Degree) Position.
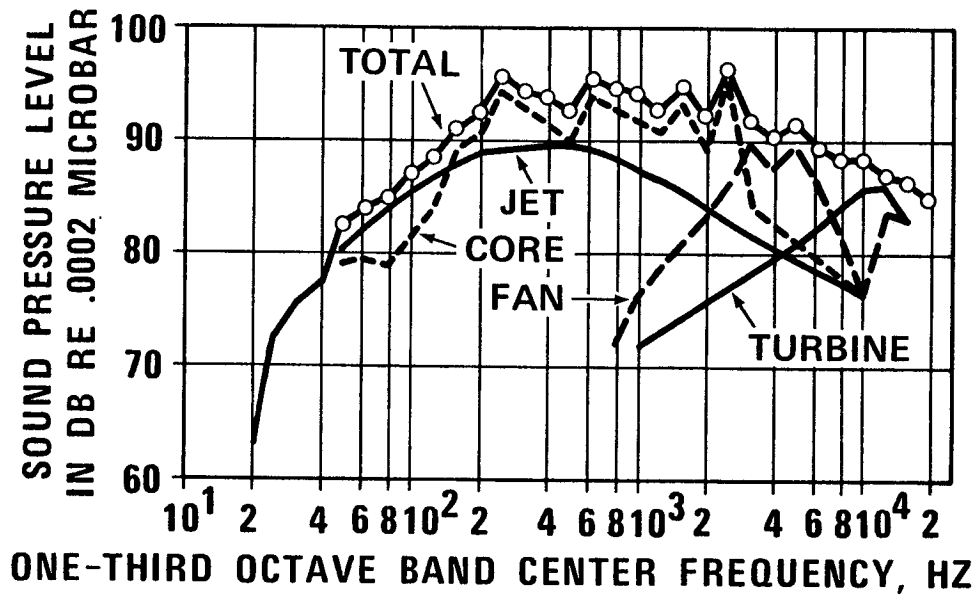
Figure 20. Data Correlation, Excess Core Model, Softwall
Mixer, 2.09-Radian (120-Degree) Position.
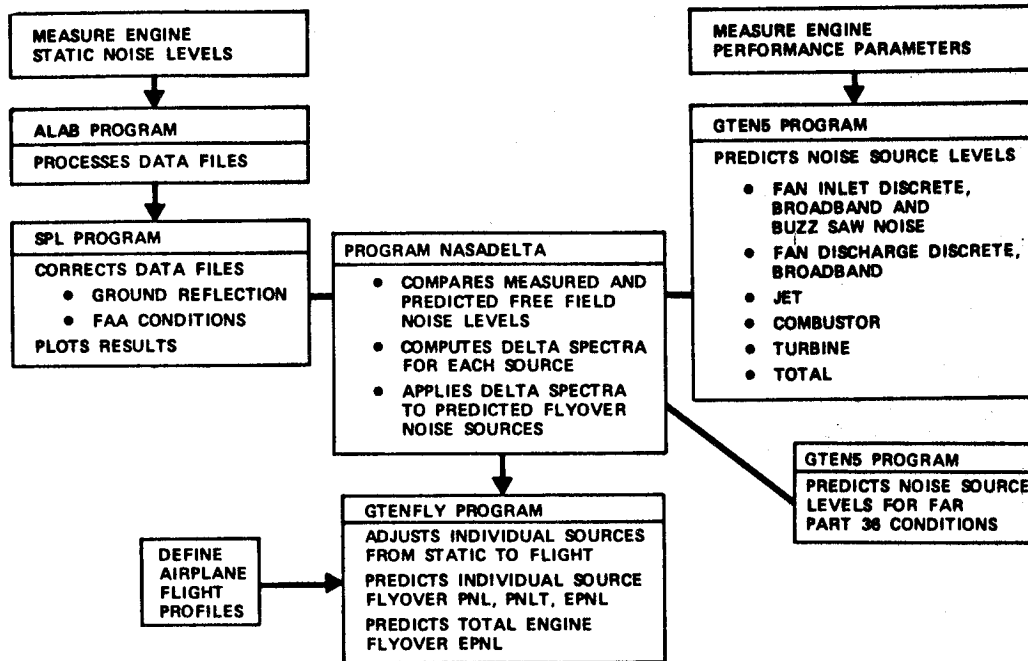
Figure 21.   Flyover Noise Prediction from Static Data.
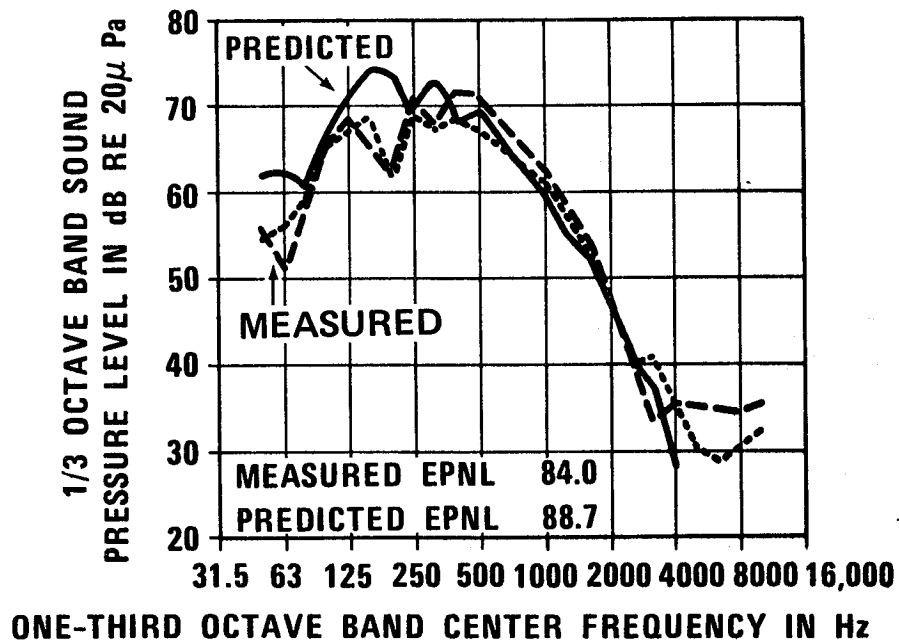
Figure 22.   Measured Learjet 35/36 versus
Predicted Excess Jet Model.
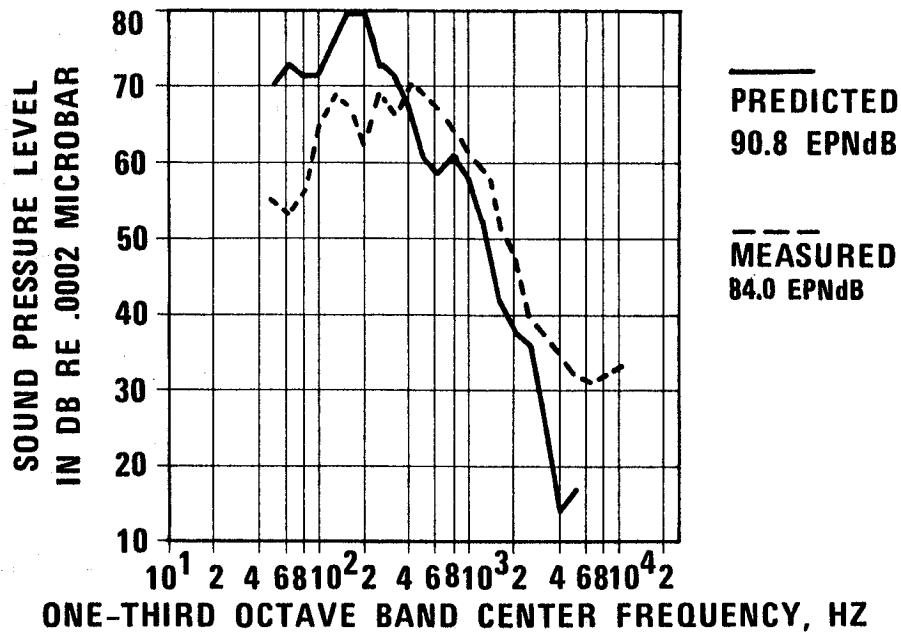
Figure 23. Measured Learjet 35/36 versus Predicted
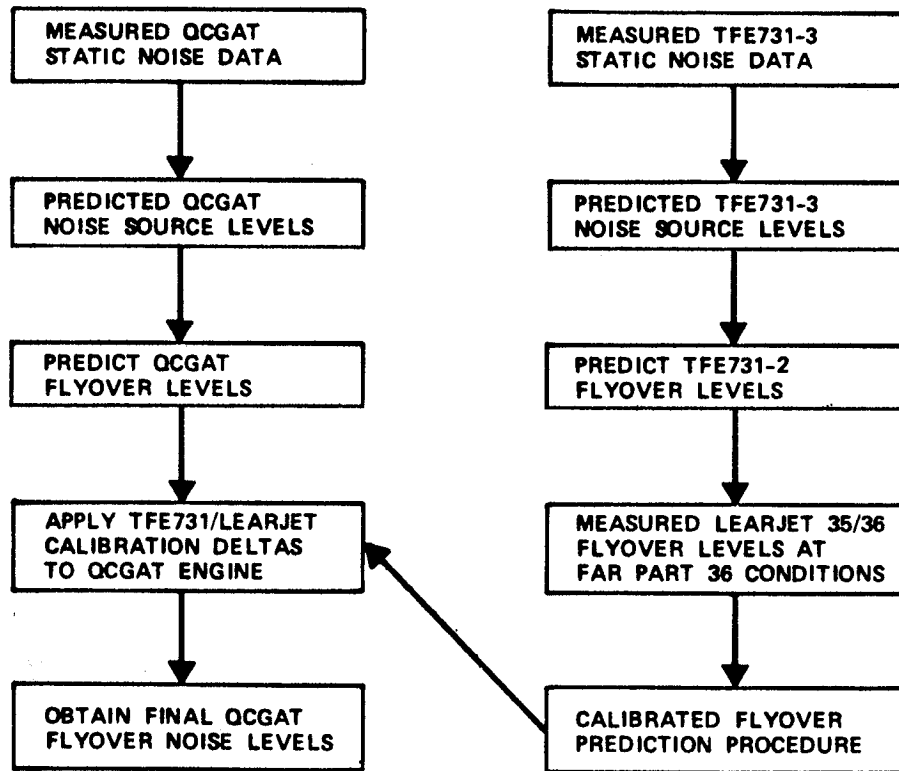Excess Core Model.
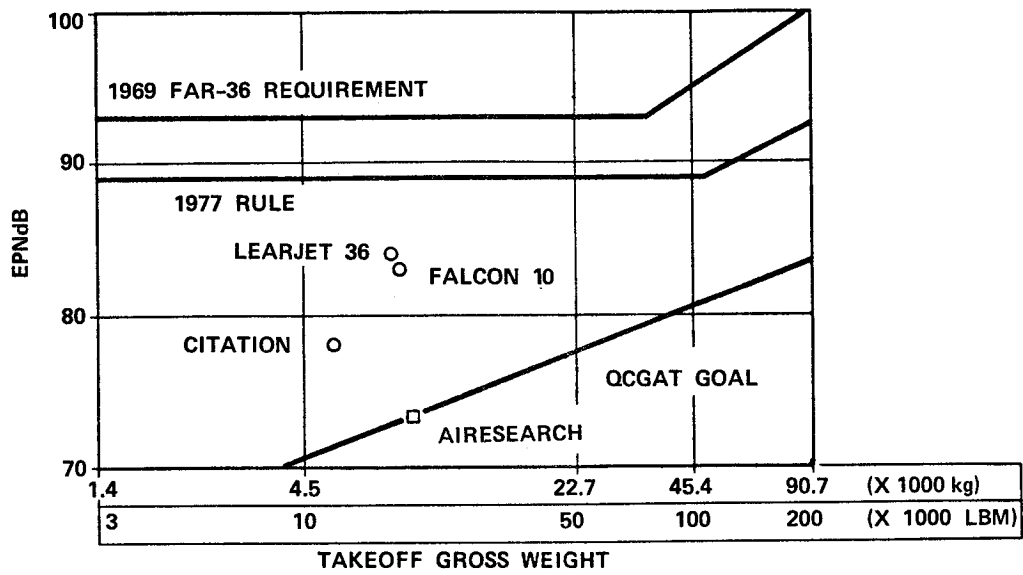

Figure 24. Flyover Noise Calibration Procedure.
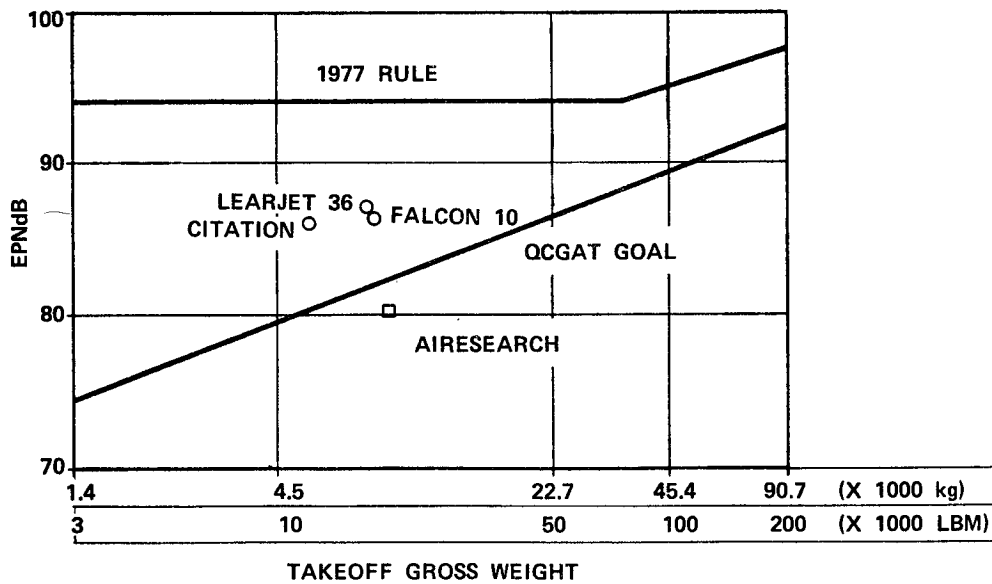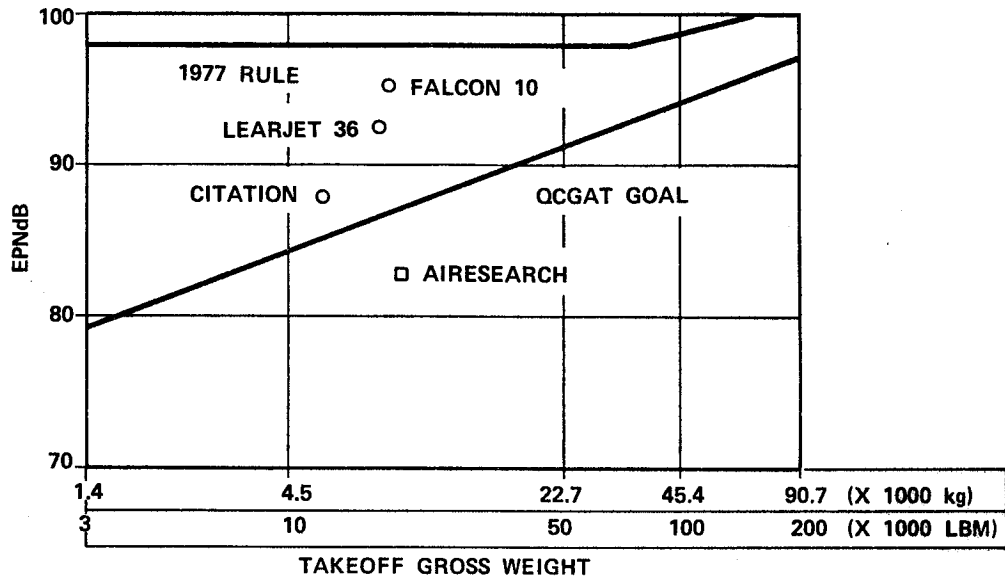
Figure 25. Takeoff Noise Summary.

Figure 26. Sideline Noise Summary.

Figure 27. Approach Noise Summary.